Journal of Molecular Modeling (2025) 31:166
https://doi.org/10.1007/s00894-025-06390-z

RESEARCH

Unraveling the influence mechanisms of different substituents on the chemical activity of N-heterocyclic phosphines via theoretical calculations

Yilei Chen[1]

Received: 17 March 2025 / Accepted: 5 May 2025

Abstract

Context N-Heterocyclic phosphines (NHP-H) represent a distinctive class of phosphorus-containing heterocycles characterized by "polarity-inverted" P–H bonds. These unique bonds facilitate a wide array of P–H reactions, rendering NHP-H compounds promising candidates for applications in organocatalysis. Although significant advancements have been made in NHP-H research, the experimental quantification of their reactivity parameters poses considerable challenges due to their high reactivity. Furthermore, the influence of various substituents on the chemical activity of NHP-H compounds remains insufficiently understood. This study examines eight NHP-H compounds with varying substituents. The findings indicate that electron-donating substituents decrease the P–H bond order, increase the negative charge on the phosphorus atom, and enhance nucleophilicity. Conversely, electron-withdrawing substituents exhibit opposite effects. Furthermore, substituents influence the local electron attachment energy of the phosphorus atom, thereby affecting reactivity in proton-transfer reactions. According to conceptual density functional theory, electron-donating substituents are associated with lower electrophilicity and higher nucleophilicity indices, whereas electron-withdrawing substituents demonstrate the opposite trend. Charge-transfer spectra suggest that electron-donating substituents reduce the excitation energy of NHP-H, thereby increasing its reactivity. Additionally, IRI analysis indicates that electron-donating substituents weaken the P–H bond, while electron-withdrawing substituents strengthen it, along with alterations in other intramolecular interactions.

Methods The study utilized the M06-2X functional in conjunction with the def2-TZVP basis set within the SMD model, employing acetonitrile as the solvent, to perform structural optimization and frequency analysis of NHP-H compounds. Computational analyses were conducted using Gaussian 09 software, with 30 excited states calculated for each compound. Multiwfn software facilitated the determination of atomic dipole moment-corrected Hirshfeld population, local electron attachment energy, the Interaction Region Indicator, and charge-transfer spectrum, which were subsequently visualized using VMD 1.9.3. Additionally, GaussView 6.0.16 software was employed to generate three-dimensional molecular configurations and prepare input files.

Keywords Substituent effects · Theoretical calculations · Chemical activity · Density functional theory

Introduction

N-Heterocyclic phosphines (NHP-H) are a class of three-coordinate phosphorus-containing heterocycles, characterized by the presence of hydrogenated P–H bonds in their structures. The "polarity inversion" exhibited by these chemical bonds leads to significant differences in the reactivity and selectivity of NHPs compared to conventional P–H acidic compounds, thereby expanding the diversity of P–H reactions [1–5].

Based on the unique structure and reaction characteristics of NHP-H, starting from the essence of its chemical bonds, the electronegativity difference plays a crucial role, providing a theoretical basis for a deeper understanding of its properties. According to the Pauling scale, the electronegativity of the phosphorus atom (P) is similar to that of the hydrogen atom. The small electronegativity difference between them provides the feasibility for regulating the polarity of the P–H bond. Until 2000, the research group of Gudat

✉ Yilei Chen
chenyilei@hezeu.edu.cn

[1] YunCheng Campus, HeZe University, HeZe 274015, China

Published online: 21 May 2025

reported the "polarity inversion" characteristic of the P–H bond in the structure of N-heterocyclic phosphine hydride reagents (N-heterocyclic phosphines (NHP-H)). Since then, the research on the hydride reactivity of NHP-H has officially commenced [6–8]. During the subsequent more than 10 years, the field has developed rapidly, and a variety of NHP-H compounds with five-membered and six-membered ring skeleton structures have been successively reported [9–13]. The emergence of these compounds provides more material basis for subsequent in-depth research and promotes the continuous development of research in this field.

NHP-H is a highly nucleophilic organic phosphane with potential as a main-group catalyst and molecular hydrogenide in organocatalytic transformations [14–16]. Its unique electronic properties and reactivity have attracted significant interest in organic chemistry. Structurally similar to nitrogen heterocyclic carbenes (NHCs), NHP-H exhibits exceptional nucleophilicity in catalytic reactions. Zhang quantified NHP-H's nucleophilicity using kinetic studies and the Mayr equation, revealing its nucleophilicity spans over 10 N units, indicating its unusual reactivity as a hydride donor. Zhang developed a nucleophilicity scale for NHP-H via kinetic studies by comparing hydrogen transfer reactions with known electrophiles using the Mayr equation. The results showed NHP-H's nucleophilicity spanned over 10 N units, indicating its unusual reactivity as hydride donors [17, 18]. Chong illustrated NHP-H's role as a catalyst in metal-free reduction of α,β-unsaturated esters and C–C bond formation with nitriles, introducing a novel strategy for C–C bond construction [19, 20].

In addition to the unique properties and extensive applications of NHP-H itself, its related derivatives also exhibit rich chemical activities, and NHP-S is a typical representative among them. NHP-S was used to reduce imine derivatives and was extended to achieve selective defluorination and hydrogenation of trifluoroalkene [21–23]. Gudat studied NHP-H's geometric structure and electronic properties, noting that phosphorus and hydrogen have similar electronegativities, resulting in low polarity in P–H bonds [24, 25]. The article highlighted the role of n(N)-σ*(P-X) hyperconjugation in P-X bond ionization polarization and discussed NHP-H's applications in catalytic cross-coupling and 1,2-disphosphine ligand synthesis [6, 7]. The P–H bond's acidity allows it to be deprotonated under basic conditions, acting as a phosphorus nucleophile for enantioselective hydrophosphorylation reactions [26–28].

Homolytic cleavage of the P–H bond forms phosphorus radicals, useful in functionalizing unsaturated bonds, particularly in photo-Arbuzov rearrangements for bioactive phosphonic acids [29, 30]. Liu used DFT calculations to explore the hydrogenide properties and catalytic potential of NHP-H, suggesting applications in catalytic silamination, silylation, and silithiolation reactions. The article also outlined NHP-H synthesis methods, including condensation/salt elimination, aminourea/diazene formation, and redox reactions with phosphorus trihalides and dipyridyl compounds, highlighting the role of P-centered bond formation and cleavage in organic synthesis [31].

The catalytic applications discussed involve forming and breaking P-centered bonds in organic synthesis. Additionally, the article covered topics such as catalytic reductions (including asymmetric variants) of carbonyl groups, imines, pyridine, and their conjugate reductions, along with further transformations induced by these reductions [32]. Alkhater calculated hydrogenide properties, reduction potentials, pKa values, and bond dissociation free energies (BDFEs) for 64 NHP-H derivatives. The results showed a wide range of hydrogenide properties and BDFEs, with NHP-H having less negative reduction potentials compared to carbon-based hydrogenides, indicating higher thermodynamic efficiency [33].

Given that the vast majority of NHPs exhibit extremely high reactivity, it can prove rather challenging to experimentally ascertain their reactivity parameters on certain occasions. In such situations, theoretical calculations emerge as a potent and supplementary means, serving to predict the reactivities of NHPs effectively [3].

Building upon the foundational work of researchers such as Zhang, who quantified the nucleophilicity of NHP-H using kinetic studies, and Gudat, who focused on the geometric and electronic properties of NHP-H, our study investigates the reactivity of NHP-H in the context of various substituents. In this work, density functional theory is applied to study eight kinds of NHP-H with different substituents, as shown in Scheme 1, aiming to reveal the influence of the substituents on the activity of NHP-H in organic catalytic reactions.

Computational details

The structural optimization and frequency analysis of eight NHP-H substituents were performed using the M06-2X [34, 35] functional and def2-TZVP [36] basis set, with acetonitrile as the solvent in the SMD model.

The optimized geometry was confirmed as a minimum by checking for the absence of imaginary frequencies. The M06-2X functional, designed for nonmetals, excels in predicting thermodynamic and kinetic properties of organic reactions, aligning well with experimental values. The def2-TZVP basis set is suitable for the main group and some transition metal elements. The properties and interactions of chemical bonds, including covalent, ionic, and metallic bonds, were accurately characterized.

For each compound, 30 excited states were computed. The keyword IOp(9/40 = 4) was employed to generate

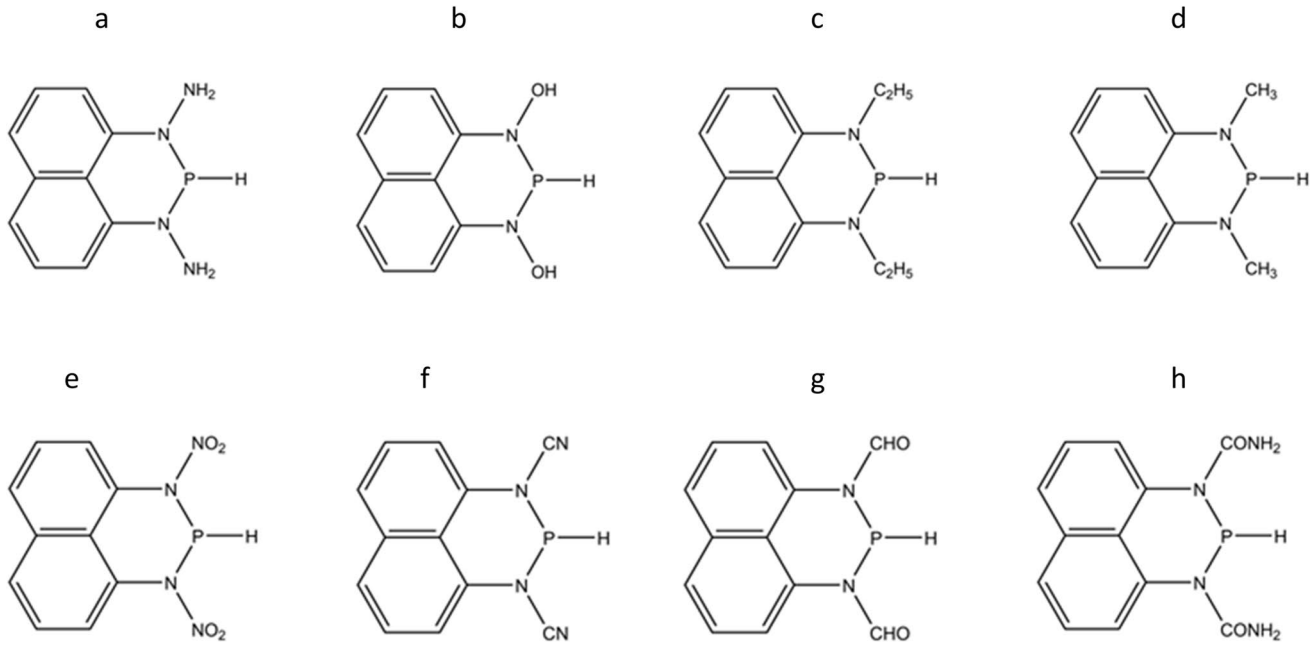

Scheme 1 The structure of NHP-H with different substituents

comprehensive configuration coefficients and ensure the accuracy of the calculations. All computational analyses were conducted using the Gaussian 09 software software [37].

Atomic dipole moment corrected Hirshfeld population, local electron attachment energy, and charge-transfer spectrum (CTS) [38] were determined utilizing the Multiwfn software [39–41] software. CTS was visualized based on the TD-DFT results. Visualization of the outcomes was facilitated by VMD 1.9.3 [42]. The three-dimensional molecular configurations and input files were prepared using Gaussview 6.0.16 software.

Bond order

The Laplacian bond order (LBO) can be calculated using the following formula [41]:

$$\mathrm{LBO}_{A,B} = -10 \times \int_{\nabla^2\rho<0} w_A(\boldsymbol{r}) w_B(\boldsymbol{r}) \nabla^2 \rho(\boldsymbol{r}) \mathrm{d}\boldsymbol{r} \tag{1}$$

where ρ(*r*) represents the electron density at a given point, and $w_{\mathrm{A}(r)}$ is an atomic weighting function that corresponds to the extent of the atomic space.

Local electron attachment energy

$$E_{\mathrm{att}}(\boldsymbol{r}) = \frac{n\sum_{i=\mathrm{LUMO}}^{\varepsilon_i<0} \left|\varphi_i(\boldsymbol{r})\right|^2 \varepsilon_i}{\rho(\boldsymbol{r})} \tag{2}$$

Here, ρ denotes the total electron density, $|\varphi_i(r)|^2$ is the probability density of the molecular orbital, and ε is the orbital energy [43].

Conceptual density functional theory

Ionization potential (IP):

$$IP = E_{N-1} - E_N \tag{3}$$

E_{N} is the energy of a system with N electrons, while $E_{\mathrm{N\text{-}1}}$ is the energy of the system after the loss of one electron.

Electron affinity (EA):

$$EA = E_N - E_{N+1} \tag{4}$$

Conversely, $E_{\mathrm{N+1}}$ represents the energy of the system after the addition of one electron.

Chemical hardness (*η*):

$$\eta = \frac{IP - EA}{2} \tag{5}$$

Chemical hardness (*S*):

$$S = \frac{2}{IP - EA} \tag{6}$$

The global electrophilicity index (ω):

$$\omega = \frac{\mu^2}{2\eta} \tag{7}$$

μ is the chemical potential:

$$\mu = -\frac{IP + EA}{2} \tag{8}$$

Nucleophilicity index (*N*):

$$N = \mu_r - \mu \tag{9}$$

μ_r is the chemical potential of the reference system.

Results and discussion

Bond order

The discussion on electron density highlights the importance of the Laplacian function, $\nabla^2\rho(r)$, which in Atoms in Molecules (AIM) theory is the sum of the three diagonal elements of the Hessian matrix of electron density at a point. A negative $\nabla^2\rho(r)$ indicates electron condensation. In chemical bond studies, a negative $\nabla^2\rho$ in the bonding region typically signifies covalent bond formation. Figure 1 shows critical points of electron density: purple, orange-yellow, and yellow represent (3, −3), (3, −1), and (3, +1) points, respectively, which are crucial for understanding electron density distribution and chemical bond formation, offering valuable insights for research [44].

The Laplacian bond order method analyzed NHP-H's chemical bonds with different substituents, as shown in Table 1. Electron-donating substituents decrease the P–H bond order, with LBO values of 0.814 for $–NH_2$, 0.828 for –OH, 0.813 for $–C_2H_5$, and 0.821 for $–CH_3$. Conversely, electron-withdrawing substituents increase the P–H bond order, with LBO values of 0.874 for $–NO_2$, 0.857 for –CN, 0.847 for –CHO, and 0.856 for $–CONH_2$. LBO values for P-N bonds were also measured, ranging from 0.523 to 0.614 for P-N1 and from 0.523 to 0.747 for P-N2, depending on the substituent.

Electron-donating substituents decrease the P–H bond order, thereby diminishing its stability and enhancing its

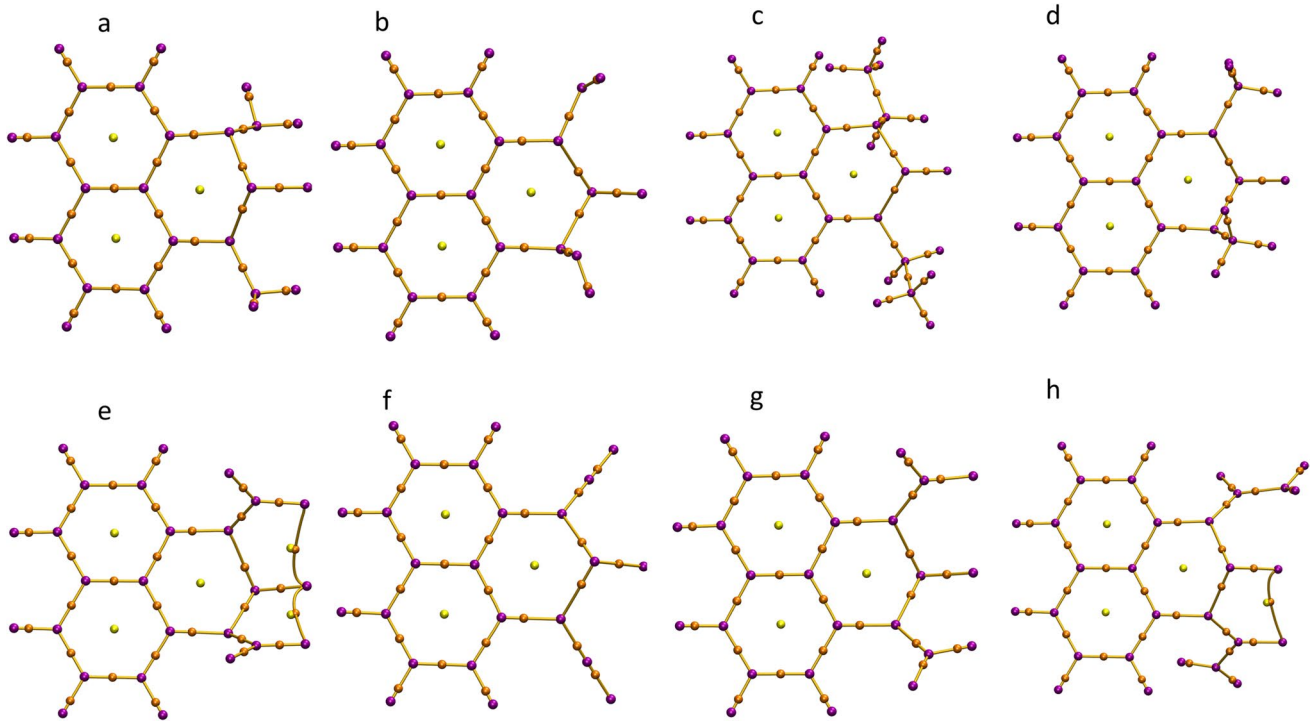

Fig. 1 AIM Topological Analysis Diagram of NHP-H with different substituents. Electron density topology of NHP-H compounds with various substituents, showing critical points (3, −3), (3, −1), and (3, +1). The distribution of these points reflects the influence of substituents on electron density and bond formation

Table 1 The LBO between the phosphorus atom and its adjacent atoms

	$–NH_2$	–OH	$–C_2H_5$	$–CH_3$	$–NO_2$	–CN	–CHO	$–CONH_2$
P–H	0.814	0.828	0.813	0.821	0.874	0.857	0.847	0.856
P-N1	0.589	0.598	0.614	0.579	0.558	0.523	0.581	0.595
P-N2	0.74	0.747	0.688	0.716	0.553	0.523	0.595	0.557

reactivity. This phenomenon is exemplified by the presence of a $–C_2H_5$ substituent, which reduces the bond order to 0.813. This observation is consistent with fundamental chemical principles, as such substituents increase the electron density around the phosphorus atom, thereby modifying the electron cloud distribution of the P–H bond [45, 46]. Conversely, electron-withdrawing groups, such as $–NO_2$, increase the bond order to 0.874, thereby augmenting the bond's stability. Electron-withdrawing groups achieve this by reducing the nucleophilicity of phosphorus through the withdrawal of its electron cloud, which results in the strengthening of the P–H bond and a concomitant decrease in its reactivity.

According to the integral formula definition, the magnitude of the Local Bond Order (LBO) value is contingent upon the degree of variation in electron density within the bond path region. A higher LBO value signifies a greater accumulation of electron density along the bond path, suggesting a more substantial contribution of electrons to the chemical bond formation, thereby indicating a stronger bond. In comparison to electron-withdrawing groups, substituents that donate electrons tend to decrease the LBO value of the phosphorus-hydrogen (P–H) bond, thereby weakening it. This weakening effect is positively correlated with the electron-donating capacity of the substituents. Conversely, electron-withdrawing groups increase the LBO value of the P–H bond, thereby enhancing its stability and reducing its reactivity.

Atomic charge

The Atomic Dipole Moment Corrected Hirshfeld Population (ADCH) method was utilized to compute the charge distributions of phosphorus (P), hydrogen (H), and nitrogen (N) atoms in NHP-H across various substituents, as outlined in Table 2.

Electron-donating groups increase the electron density and induce a negative charge on the phosphorus (P) atom, with ADCH charge values of −0.0300 for $–NH_2$, 0.0007 for –OH, −0.1102 for $–C_2H_5$, and −0.1029 for $–CH_3$. In contrast, electron-withdrawing groups decrease electron density, leading to a positive charge, with values of 0.1556 for $–NO_2$, 0.1439 for –CN, 0.0058 for –CHO, and −0.0169 for $–CONH_2$. Similar effects are observed on adjacent nitrogen (N) atoms. For N1, the values are −0.0806 with $–NH_2$, −0.0892 with –OH, −0.1025 with $–C_2H_5$, and −0.0056 with $–NO_2$. For N2, the values are −0.0248 with $–NH_2$, −0.0583 with –OH, −0.1153 with $–C_2H_5$, and 0.0135 with $–NO_2$The influence of various substituents on hydrogen atoms is minimal, as evidenced by the slight fluctuations in the ADCH charge values of these atoms across different substituents. For instance, when the substituent is $–NH_2$, the charge value is 0.1560; for –OH, it is 0.1415; for $–C_2H_5$, it is 0.1607; and for $–NO_2$, it is 0.1502.

The distribution of atomic charges reveals that electron-donating substituents confer a negative charge on the phosphorus atom, thereby enhancing its nucleophilicity, whereas electron-withdrawing substituents impart a positive charge, diminishing its nucleophilicity [47]. For example, an ethyl group ($–C_2H_5$) results in a phosphorus charge of −0.1102, while a nitro group ($–NO_2$) leads to a charge of 0.1556. This variation in charge significantly influences the nucleophilic behavior of NHP-H, as a negatively charged phosphorus is more inclined to engage with positively charged sites. Electron-donating groups amplify this propensity, whereas electron-withdrawing groups attenuate it. Furthermore, substituents similarly affect the charge of adjacent nitrogen atoms but exert minimal influence on hydrogen atoms, indicating that electronic effects are predominantly transmitted through directly bonded atoms.

Local electron attachment energy

Additionally, a minimum value of the local electron attachment energy (LEAE) is observed at the phosphorus atom, as illustrated in Fig. 2.

Among the electron-donating substituents, the hydroxyl group (–OH) exhibits the most negative local electron affinity energy (LEAE) value, measured at −0.77 eV. The LEAE value for the amino group ($–NH_2$) is approximately −0.05 eV, which is nearly neutral, although this value may be refined with more precise data. The ethyl ($–C_2H_5$) and methyl ($–CH_3$) groups have LEAE values of −0.03 eV and −0.04 eV, respectively. Conversely, within the electron-withdrawing substituents, the cyano group (–CN) displays the most negative LEAE value at −0.57 eV, followed by the nitro group ($–NO_2$) at −0.47 eV, the formyl group (–CHO) at −0.31 eV, and the amide group ($–CONH_2$) at −0.23 eV.

The minimum local electron attachment energy (LEAE) at the phosphorus atom, along with the impact of various

Table 2 Atomic charges calculated with ADCH

	$–NH_2$	–OH	$–C_2H_5$	$–CH_3$	$–NO_2$	–CN	–CHO	$–CONH_2$
P	− 0.0300	0.0007	− 0.1102	− 0.1029	0.1556	0.1439	0.0058	− 0.0169
H	0.1560	0.1415	0.1607	0.1632	0.1502	0.1715	0.1514	0.1456
N1	− 0.0806	− 0.0892	− 0.1025	− 0.1448	− 0.0056	0.0254	− 0.0166	− 0.1275
N2	− 0.0248	− 0.0583	− 0.1153	− 0.0592	0.0135	0.0254	0.0791	− 0.1816

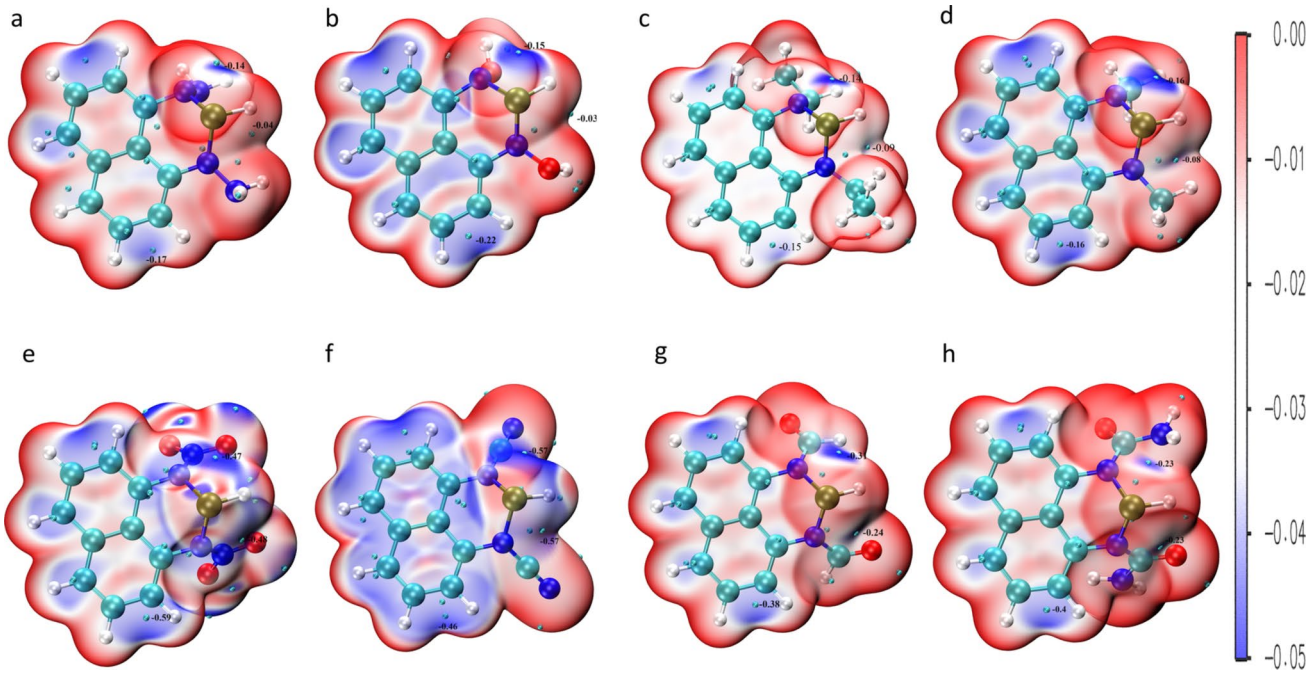

Fig. 2 Local electron attachment energy (LEAE) at the phosphorus atom for NHP-H compounds with various substituents. LEAE values indicate the impact of substituents on the nucleophilic properties of NHP-H

substituents, elucidates the regulatory role these substituents play in modulating the protophilic activity of NHP-H molecules [48]. The hydroxyl (–OH) group, functioning as an electron donor, exhibits the lowest LEAE value of − 0.77 eV, indicating its potential to enhance binding affinity towards protophilic reagents. Conversely, the cyano (–CN) group, an electron acceptor, also demonstrates significant protophilic activity with an LEAE of − 0.57 eV. Therefore, in proton transfer reactions, NHP-H molecules with diverse substituents will display differential selectivities and activities contingent upon their LEAE values, with more negative LEAE values favoring proton attraction and facilitating reaction promotion.

Conceptual density functional theory

The parameters, including ionization potential (IP), electron affinity (EA), chemical hardness (η), softness (*S*), global electrophilicity index (ω), and nucleophilicity index (*N*) of NHP-H with various substituents, were computed and are presented in Table 3.

The electrophilicity indices of electron-donating substituents, such as $–NH_2$, –OH, $–C_2H_5$, and $–CH_3$, are significantly lower than those of electron-withdrawing substituents. Specifically, the electrophilicity index values for $–NH_2$, –OH, $–C_2H_5$, and $–CH_3$ are 0.5543 eV, 0.6326 eV, 0.5505 eV, and 0.5595 eV, respectively. In contrast, the electrophilicity index for the electron-withdrawing substituent $–NO_2$ is substantially higher at 1.2029 eV. Conversely, the

Table 3 The reactivity descriptor of NHP-H with different substituents

	IP (eV)	EA (eV)	η (eV)	*S* (eV^{-1})	ω (eV)	*N* (eV)
$–NH_2$	6.5388	− 0.8245	7.3632	0.1358	0.5543	4.2466
–OH	6.8021	− 0.6576	7.4597	0.1341	0.6326	4.0120
$–C_2H_5$	6.4545	− 0.8014	7.2559	0.1378	0.5505	4.2611
$–CH_3$	6.5814	− 0.8241	7.4054	0.1350	0.5595	4.1850
$–NO_2$	8.1127	0.4657	7.6470	0.1308	1.2029	2.6539
–CN	7.7824	0.3853	7.3971	0.1352	1.1273	2.9412
–CHO	7.6166	0.0407	7.5759	0.1320	0.9674	3.1371
$–CONH_2$	7.2210	− 0.2310	7.4521	0.1342	0.8196	3.4975

nucleophilicity indices for the electron-donating substituents are relatively high, with values of 4.2466 eV for $–NH_2$, 4.0120 eV for –OH, 4.2611 eV for $–C_2H_5$, and 4.1850 eV for $–CH_3$. Additionally, there are notable differences in the ionization potentials (IP) among the substituents, with values of 6.5388 eV for $–NH_2$, 6.8021 eV for –OH, and 8.1127 eV for $–NO_2$. Regarding electron affinity (EA), the values are − 0.8245 eV for $–NH_2$, − 0.6576 eV for –OH, and 0.4657 eV for $–NO_2$.

This study utilizes MultiWFN to compute the condensed local electrophilicity/nucleophilicity index. Figure 3 presents the corresponding values for phosphorus atoms, indicating that electron-donating groups demonstrate a heightened affinity for electron-withdrawing substituents. Among the substituents examined, the hydroxyl group (–OH) exhibits the highest condensed local electrophilicity/nucleophilicity index at 0.4457 eV, whereas the nitro group ($–NO_2$), a potent electron-withdrawing substituent, possesses the lowest value at 0.1345 eV.

Conceptual density functional theory (DFT) calculations provide insights into the chemical reactivity of NHP-H when modified with various substituents [49–51]. Quantitative parameters, such as electrophilicity and nucleophilicity indices, are employed to assess the influence of these substituents on the electron-donating and electron-accepting properties of NHP-H [52, 53]. Substituents that donate electrons typically exhibit lower electrophilicity and higher nucleophilicity indices, thereby enhancing their propensity to donate electrons during chemical reactions. Conversely, electron-withdrawing substituents, exemplified by $–NO_2$ with an electrophilicity index of 1.2029 eV, are more inclined to accept electrons. These parameters are instrumental in elucidating the reactivity of NHP-H in various chemical contexts and facilitate the prediction of reaction outcomes.

Charge-transfer spectrum

Using time-dependent density functional theory (TDDFT), 30 excited states of NHP-H with different substituents were calculated, with the first excited state (S1) energies shown in Fig. 4. The amino group substitution has the lowest S1 energy at 3.4089 eV, while the aldehyde group substitution has the highest at 3.8291 eV. Other S1 energies are –OH at 3.5012 eV, $–C_2H_5$ at 3.4567 eV, $–CH_3$ at 3.4325 eV, $–NO_2$ at 3.7568 eV, –CN at 3.7023 eV, and $–CONH_2$ at 3.6015 eV.

The CTS analysis utilizes the interfragment charge transfer approach to examine electron transfer dynamics between any two fragments of the system during electronic excitation, as depicted in Fig. 5.

The charge-transfer spectrum analysis indicates that NHP-H molecules substituted with electron-donating groups demonstrate lower excitation energies and increased reactivity [54, 55]. Moreover, these substitutions lead to a decrease in electron transfer from Fragment 1 to Fragment 2. For example, when comparing NHP-H molecules substituted with an amino group to those with an aldehyde group, within a specific wavelength range (e.g., 200–400 nm), the intensity of the electron transfer contribution peak from Fragment 1 to Fragment 2 is significantly lower in the amino group-substituted NHP-H than in its aldehyde group-substituted counterpart.

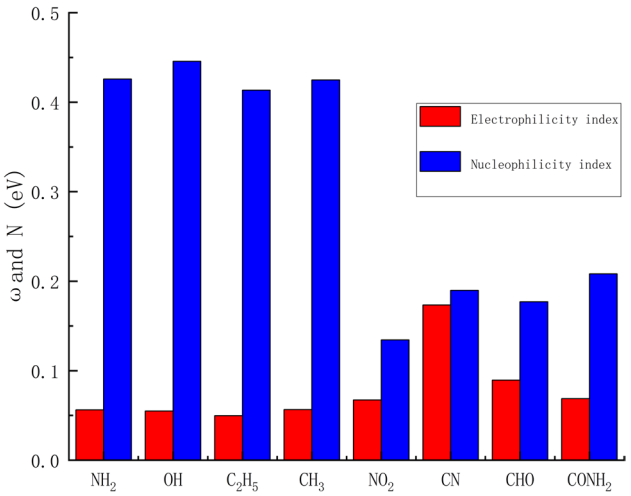

Fig. 3 Condensed local electrophilicity/nucleophilicity indices for phosphorus atoms in NHP-H compounds with different substituents. The indices highlight the contrasting effects of electron-donating and electron-withdrawing groups on the reactivity of the phosphorus center

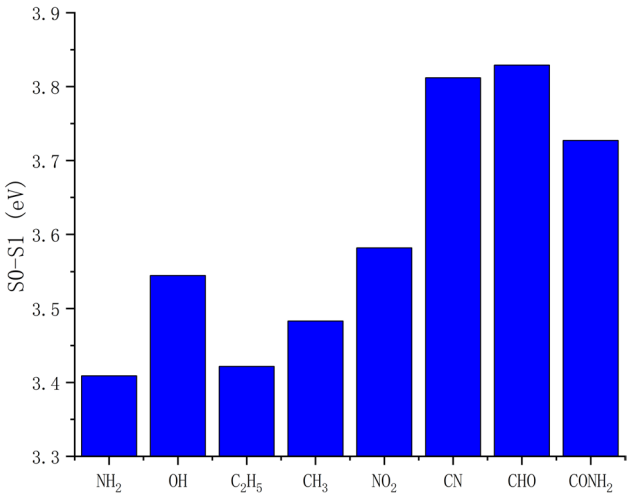

Fig. 4 First excited state (S1) energies of NHP-H compounds with various substituents. The variation in excitation energies reflects the influence of different substituents on the electronic excitation properties of NHP-H

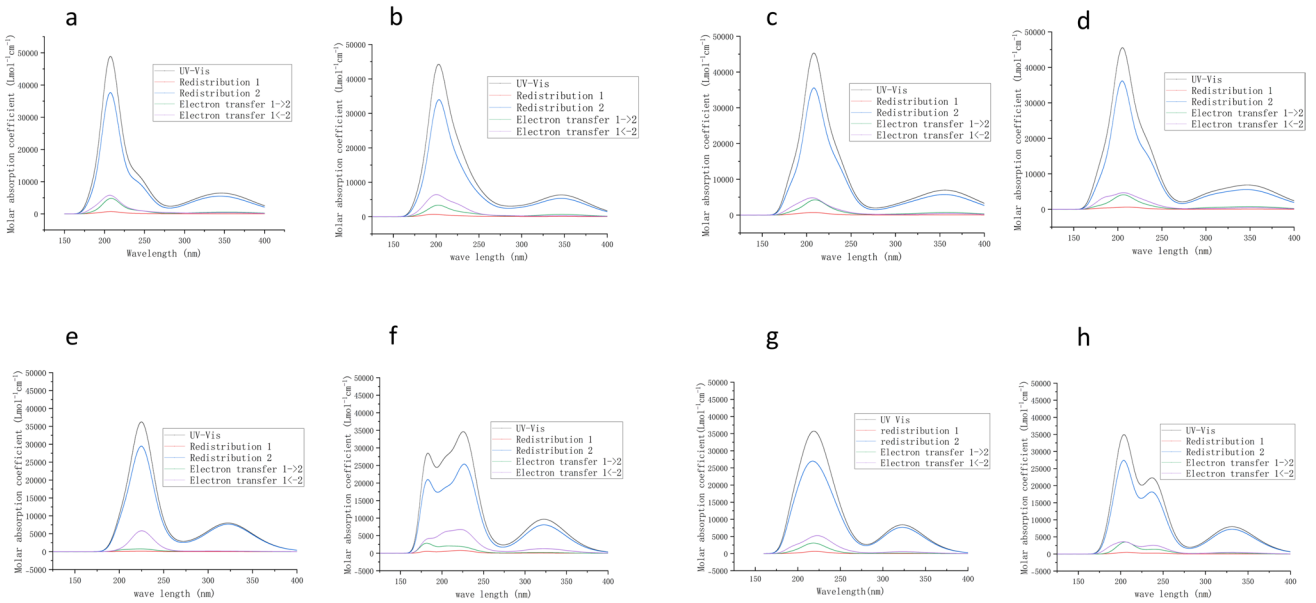

Fig. 5 Charge-transfer spectra of NHP-H compounds with different substituents, illustrating the dynamics of electron transfer between molecular fragments upon electronic excitation. The spectra highlight differences in electron transfer contributions due to the nature of the substituents

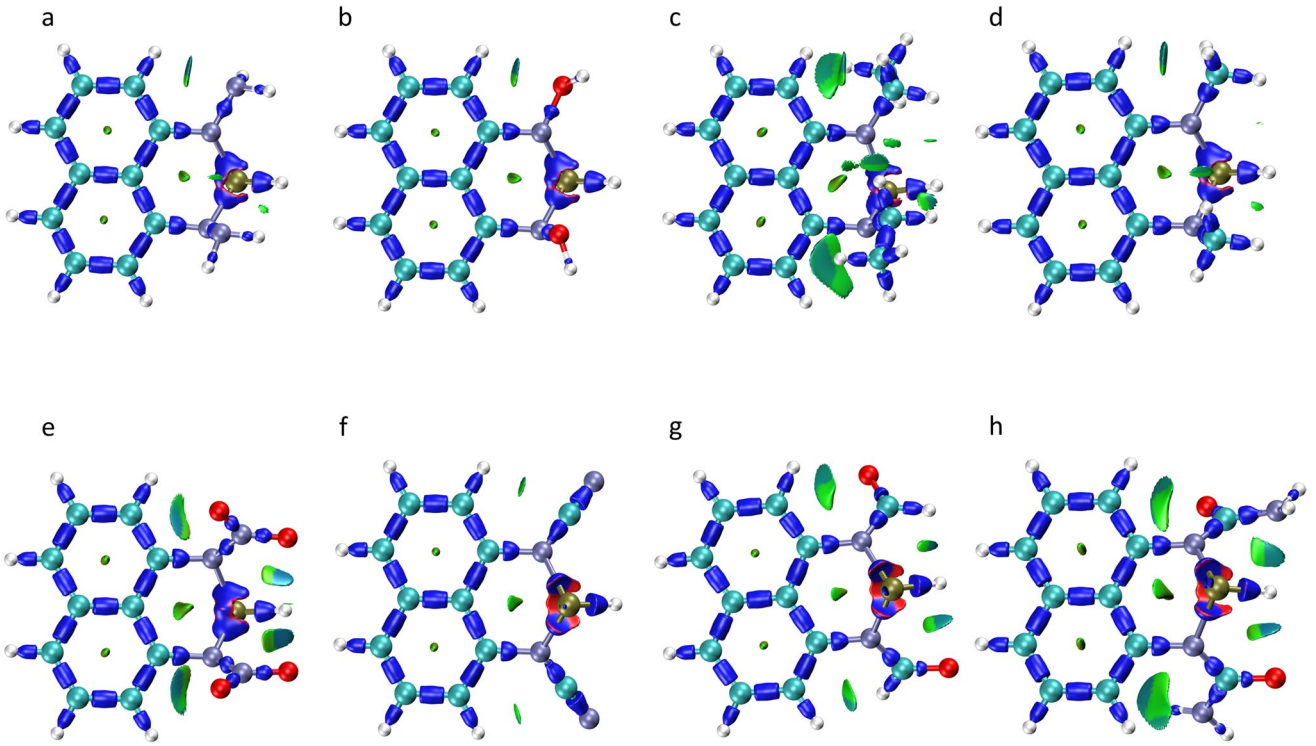

Fig. 6 Interaction region indicator (IRI) analysis of NHP-H compounds with various substituents, revealing the distribution and strength of chemical bonds and weak interactions within the molecules. The IRI spectra highlight how electron-donating and electron-withdrawing groups alter the electron density around the phosphorus atom, affecting the stability and reactivity of the P–H bonds

Interaction region indicator

IRI allows for the intuitive revelation of chemical bonds and weak interactions within chemical systems. Compared with other methods for weak interactions, the advantage of IRI lies in its ability to display all types of interactions equally [56].

This study used the IRI method to analyze NHP-H molecules with various substituents. The findings indicate that electron-donating substituents alter chemical bonds and weak interactions by increasing electron cloud density around the phosphorus atom. This affects the electron distribution and interaction strength in the P–H bond region, as seen in Fig. 6. These changes align with previous Laplacian bond order (LBO) results, showing that such substituents lower the LBO value, reducing P–H bond stability and increasing reactivity, which is reflected as bond weakening in the IRI spectrum. IRI indicates that electron-withdrawing substituents enhance the stability of the P–H bond in NHP-H molecules by drawing electrons away from phosphorus. This results in a distinct interaction pattern in the IRI spectrum, showing increased interaction strength and improved bond stability, as reflected by a higher LBO value, compared to systems with electron-donating substituents. IRI can reveal various chemical bonds and weak interactions in NHP-H molecules beyond the P–H bond. For instance, the P-N bond's interaction characteristics change with different substituents. The IRI spectrum allows for intuitive observation of electron distribution changes in the P-N bond region, reflecting how substituents influence nitrogen atom charges and affect other molecular interactions by altering electron cloud distribution. IRI analysis offers a clear and thorough view of the structure and reactivity of NHP-H molecules influenced by various substituents. It enhances other calculations like bond order and atomic charge, shedding light on how substituents affect chemical activity. This visualization method aids in understanding intramolecular interactions, informs future research on NHP-H organocatalytic reactions, and supports the design and optimization of NHP-H catalysts for targeted reactions.

Conclusions

This study utilizes theoretical calculations to examine the influence of various substituents on the chemical reactivity of NHP-H. The results demonstrate that electron-donating substituents decrease the P–H bond order, impart a negative charge to the phosphorus atom, and enhance its nucleophilicity. In contrast, electron-withdrawing substituents produce opposite effects. These substituents affect the local electron attachment energy of the phosphorus atom, thereby modulating the reactivity of NHP-H in proton transfer reactions. According to conceptual density functional theory, electron-donating substituents are characterized by low electrophilicity and high nucleophilicity, whereas electron-withdrawing substituents exhibit the opposite properties. Charge-transfer spectra indicate that electron-donating substituents reduce the excitation energy of NHP-H, thus increasing its reactivity. Furthermore, IRI analysis reveals that electron-donating substituents weaken the P–H bond, whereas electron-withdrawing substituents strengthen it. IRI analysis also provides insights into changes in other intramolecular interactions. This study provides a theoretical foundation for the application of NHP-H in organocatalysis.

Author Contribution All the work of this article was completed by Yilei Chen.

Funding This research was funded by The Doctoral Research Startup Fund of Heze University, grant number XY22BS40.

Data Availability No datasets were generated or analysed during the current study.

Declarations

Competing interests The authors declare no competing interests.

References

1. Zhang YS, Huan Z, Yang JD, Cheng JP (2022) Synthetic applications of NHPs: from the hydride pathway to a radical mechanism. Chem Commun 58(90):12528–12543. https://doi.org/10.1039/D2CC04844B
2. Johannes K (2024) New applications of 1,3,2-diazaphospholenes in catalysis. EPFL. https://doi.org/10.5075/epfl-thesis-10716
3. Xu K, Zhang YS, Zhong B, Zhang L, Yang JD, Luo SZ (2024) Organocatalytic hydrogen evolution reaction by diazaphospholenes. J Am Chem Soc 146(38):25956–25962. https://doi.org/10.1021/jacs.4c10302
4. Howard MP, Miura-Akagi PM, Chapp TW, Ah-Tye YJH, Kitano T, Zhou DY, Balkwill LG, Yoshida WY, Fuller AL, Yap GPA, Rheingold AL, Borosky GL, Laali KK, Cain MF (2024) Synthesis and reactivity of a P-H functionalized benzazaphosphole.

Polyhedron 253:116905. https://doi.org/10.1016/j.poly.2024.116905
5. Zhang GT, Wodrich MD, Cramer N (2024) Catalytic enantioselective reductive Eschenmoser-Claisen rearrangements. Science 383(6681):395–401. https://doi.org/10.1126/science.adl3369
6. Gudat D (2010) Diazaphospholenes: N-heterocyclic phosphines between molecules and Lewis pairs. Acc Chem Res 43(10):1307–1316. https://doi.org/10.1021/ar100041j
7. Gupta N (2010) Recent advances in the chemistry of diazaphospholes. In: Phosphorus Heterocycles II. Springer, Berlin, Heidelberg, pp 175–206. https://doi.org/10.1007/7081_2009_20
8. Gudat D, Haghverdi A, Hupfer H, Nieger M (2000) Stability and electrophilicity of phosphorus analogues of Arduengo carbenes-an experimental and computational study. Chem Eur J 6(18):3414–3425. https://doi.org/10.1002/1521-3765(20000915)6:18%3c3414::AID-CHEM3414%3e3.0.CO;2-P
9. Zhang JJ, Yang JD, Cheng JP (2020) Diazaphosphinanes as hydride, hydrogen atom, proton or electron donors under transition-metal-free conditions: thermodynamics, kinetics, and synthetic applications. Chem Sci 11(14):3672–3679. https://doi.org/10.1039/C9SC05883D
10. Compagno N, Piccolo R, Bortolamiol E, Demitri N, Rizzolio F, Visentin F, Scattolin T (2024) Platinum(0)-η^2-1,2-(E)ditosylethene complexes bearing phosphine, isocyanide and N-heterocyclic carbene ligands: synthesis and cytotoxicity towards ovarian and breast cancer cells. Molecules 29(5):1119. https://doi.org/10.3390/molecules29051119
11. Kumar SA, Das B, Jyoti PS, Shekhar PC, Doddi A (2024) N-Heterocyclic olefin-phosphines based cationic ruthenium complexes as pre-catalysts for dual C-H bond functionalizations. Adv Synth Catal 366(11):2468–2476. https://doi.org/10.1002/adsc.202400083
12. Yousefshahi MR, Cheraghi M, Ghasemi T, Neshat A, Eigner V, Dusek M, Amjadi M, Akbari-Birgani S (2024) N-Heterocyclic carbene-Au(I)-phosphine complexes: characterization, theoretical structure analysis, and anti-cancer properties. Organometallics 43(23):3031–3042. https://doi.org/10.1021/acs.organomet.4c00405
13. Feil CM, Goerigk F, Stöckl Y, Nieger M, Gudat D (2025) Diverse reactivity of a cationic N-heterocyclic phosphenium complex towards anionic substrates-substitution vs reduction. Dalton transactions 54(5):1806–1814. https://doi.org/10.1039/D4DT03352C
14. Miaskiewicz S, Reed JH, Donets PA, Oliveira CC, Cramer N (2018) Chiral 1,3,2-diazaphospholenes as catalytic molecular hydrides for enantioselective conjugate reductions. Angew Chem Int Ed 57(15):4039–4042. https://doi.org/10.1002/anie.201801300
15. Riley R, Huchenski B, Bamford K, Speed A (2022) Diazaphospholene-catalyzed radical reactions from aryl halides. Angew Chem Int Ed 61(30):e202204088 https://doi.org/10.26434/chemrxiv-2022-4knjf
16. Huchenski BSN, Robertson KN (2020) Speed AWH (2020) Functionalization of bis-diazaphospholene P-P bonds with diverse electrophiles. Eur J Org Chem 32:5140–5144. https://doi.org/10.1002/ejoc.202000880
17. Zhang JJ, Yang JD, Cheng JP (2021) Recent progress in reactivity study and synthetic application of N-heterocyclic phosphorus hydrides. Natl Sci Rev 8(4):nwaa253. https://doi.org/10.1093/nsr/nwaa253
18. Zhang JJ, Yang JD, Cheng JP (2019) A nucleophilicity scale for the reactivity of diazaphospholenium hydrides: structural insights and synthetic applications. Angew Chem Int Ed 58(18):5983–5987. https://doi.org/10.1002/anie.201901456
19. Chong CC, Kinjo R (2015) Hydrophosphination of CO_2 and subsequent formate transfer in the 1,3,2-diazaphospholene-catalyzed N-formylation of amines. Angew Chem Int Ed 54(41):12116–12120. https://doi.org/10.1002/anie.201505244
20. Chong CC, Rao B, Kinjo R (2017) Metal-free catalytic reduction of α, β-unsaturated esters by 1,3,2-diazaphospholene and subsequent C-C coupling with nitriles. ACS Catal 7(9):5814–5819. https://doi.org/10.1021/acscatal.7b01338
21. Lin YC, Hatzakis E, Mccarthy SM, Reichl KD, Lai TY, Yennawar HP, Radosevich AT (2017) P-N cooperative borane activation and catalytic hydroboration by a distorted phosphorous triamide platform. J Am Chem Soc 139(16):6008–6016. https://doi.org/10.1021/jacs.7b02512
22. Rao B, Chong CC, Kinjo R (2018) Metal-free regio- and chemoselective hydroboration of pyridines catalyzed by 1,3,2-diazaphosphenium triflate. J Am Chem Soc 140(2):652–656. https://doi.org/10.1021/jacs.7b09754
23. Lundrigan T, Welsh EN, Hynes T, Tien CH, Adams MR, Roy KR, Robertson KN, Speed AWH (2019) Enantioselective imine reduction catalyzed by phosphenium ions. J Am Chem Soc 141(36):14083–14088. https://doi.org/10.1021/jacs.9b07293
24. Zhang JJ, Yang JD, Cheng JP (2021) Chemoselective catalytic hydrodefluorination of trifluoromethylalkenes towards mono-/gem-di-fluoroalkenes under metal-free conditions. Nat Commun 12(1):2835. https://doi.org/10.1038/s41467-021-23101-3
25. Zhang JJ, Zhao X, Yang JD, Cheng JP (2022) Diazaphospholene-catalyzed hydrodefluorination of polyfluoroarenes with phenylsilane via concerted nucleophilic aromatic substitution. J Org Chem 87(1):294–300. https://doi.org/10.1021/acs.joc.1c02360
26. Longeau A, Knochel P (1996) Lithiated bis(diethylamino)phosphine borane complex as useful nucleophilic phosphorus reagent. Tetrahedron Lett 37(34):6099–6102. https://doi.org/10.1016/0040-4039(96)01296-8
27. Sadow AD, Togni A (2005) Enantioselective addition of secondary phosphines to methacrylonitrile: catalysis and mechanism. J Am Chem Soc 127(48):17012–17024. https://doi.org/10.1021/ja0555163
28. Blum M, Kappler J, Schlindwein SH, Nieger M, Gudat D (2018) Synthesis, spectroscopic characterisation and transmetalation of lithium and potassium diaminophosphanide-boranes. Dalton Trans 47(1):112–119. https://doi.org/10.1039/C7DT04110A
29. Marque S, Tordo P (2005) Reactivity of phosphorus centered radicals. In: New Aspectsin Phosphorus Chemistry V. Springer, Berlin, Heidelberg, pp 43–76. https://doi.org/10.1007/b100981
30. Gao YZ, Tang G, Zhao YF (2018) Recent advances of phosphorus-centered radical promoted difunctionalization of unsaturated carbon-carbon bonds. Chin J Org Chem 38(1):62–74. https://doi.org/10.6023/cjoc201708023
31. Liu LL, Wu YL, Chen P, Chan CL, Xu J, Zhu J, Zhao Y (2016) Mechanism, catalysis and predictions of 1,3,2-diazaphospholenes: theoretical insight into highly polarized P-X bonds. Org Chem Front 3(4):423–433. https://doi.org/10.1039/c6qo00002a
32. Speed AWH (2020) Applications of diazaphospholene hydrides in chemical catalysis. Chem Soc Rev 49(22):8335–8353. https://doi.org/10.1039/D0CS00476F
33. Alkhater MF, Alherz AW, Musgrave CB (2021) Diazaphospholenes as reducing agents: a thermodynamic and electrochemical DFT study. Phys Chem Chem Phys 23(33):17794–17802. https://doi.org/10.1039/d1cp02193a
34. Zhao Y, Truhlar DG (2008) The M06 suite of density functionals for main group thermochemistry, thermochemical kinetics, noncovalent interactions, excited states, and transition elements: two new functionals and systematic testing of four M06-class functionals and 12 other functionals. Theor Chem Acc 120(1):215–241. https://doi.org/10.1007/s00214-007-0310-x
35. Walker M, Harvey AJA, Sen A, Dessent CEH (2013) Performance of M06, M06–2X, and M06-HF density functionals for conformationally flexible anionic clusters: M06 functionals perform better than B3LYP for a model system with dispersion and ionic

hydrogen-bonding interactions. J Phys Chem A 117(47):12590–12600. https://doi.org/10.1021/jp408166m
36. Weigend F, Ahlrichs R (2005) Balanced basis sets of split valence, triple zeta valence and quadruple zeta valence quality for H to Rn: Design and assessment of accuracy. Phys Chem Chem Phys 7(18):3297–3305. https://doi.org/10.1039/B508541A
37. Frisch MJ, Trucks GW, Schlegel HB, Scuseria GE, Robb MA, Cheeseman JR, Scalmani G, Barone V, Petersson GA, Nakatsuji H, Li X, Caricato M, Marenich AV, Bloino J, Janesko BG, Gomperts R, Mennucci B, Hratchian HP, Ortiz JV, Izmaylov AF, Sonnenberg JL, Williams, Ding F, Lipparini F, Egidi F, Goings J, Peng B, Petrone A, Henderson T, Ranasinghe D, Zakrzewski VG, Gao J, Rega N, Zheng G, Liang W, Hada M, Ehara M, Toyota K, Fukuda R, Hasegawa J, Ishida M, Nakajima T, Honda Y, Kitao O, Nakai H, Vreven T, Throssell K, Montgomery JA, Peralta JE, Ogliaro F, Bearpark MJ, Heyd JJ, Brothers EN, Kudin KN, Staroverov VN, Keith TA, Kobayashi R, Normand J, Raghavachari K, Rendell AP, Burant JC, Iyengar SS, Tomasi J, Cossi M, Millam JM, Klene M, Adamo C, Cammi R, Ochterski JW, Martin RL, Morokuma K, Farkas O, Foresman JB, Fox D J (2009) Gaussian 09 Rev. C.01 [Z]. Wallingford, CT.
38. Liu ZY, Wang X, Lu T, Yuan AH, Yan XF (2022) Potential optical molecular switch: lithium@cyclo[18]carbon complex transforming between two stable configurations. Carbon 187:78–85. https://doi.org/10.1016/j.carbon.2021.11.005
39. Lu T, Chen FW (2012) Multiwfn: a multifunctional wavefunction analyzer. J Comput Chem 33(5):580–592. https://doi.org/10.1002/jcc.22885
40. Lu T, Chen FW (2012) Atomic dipole moment corrected hirshfeld population method. JTheor Comput Chem 11(01):163–183. https://doi.org/10.1142/S0219633612500113
41. Lu T, Chen FW (2013) Bond order analysis based on the laplacian of electron density in fuzzy overlap space. J Phys Chem A 117(14):3100–3108. https://doi.org/10.1021/jp4010345
42. Humphrey W, Dalke A, Schulten K (1996) VMD: visual molecular dynamics. J Mol Graph 14(1):33–38. https://doi.org/10.1016/0263-7855(96)00018-5
43. Brinck T, Carlqvist P, Stenlid JH (2016) Local electron attachment energy and its use for predicting nucleophilic reactions and halogen bonding. J Phys Chem A 120(50):10023–10032. https://doi.org/10.1021/acs.jpca.6b10142
44. Bader RFW (1985) Atoms in molecules. Acc Chem Res 18(1):9–15. https://doi.org/10.1021/ar00109a003
45. Cheng XL, Li F, Zhao YY, Cheng XY, Nie K, Han YF, Yang YJ (2022) Stability, atomic charges, bond-order analysis, and the directionality of lone-electron pairs on nitriles and isocyanides. J Phys Org Chem 35(12):e4420. https://doi.org/10.1002/poc.4420
46. Zhang E, Hirao H (2024) Exploring the bonding nature of iron(IV)-oxo species through valence bond calculations and electron density analysis. J Phys Chem A 128(34):7167–7176. https://doi.org/10.1021/acs.jpca.4c04335
47. Carmona-Espíndola J, Gázquez JL (2023) Study of a smooth interpolation between Hirshfeld and iterative Hirshfeld population analyses. Comput Theor Chem 1229:114335. https://doi.org/10.1016/j.comptc.2023.114335
48. Lu J, Paci I, Leitch DC (2022) A broadly applicable quantitative relative reactivity model for nucleophilic aromatic substitution (SNAr) using simple descriptors. Chem Sci 13(43):12681–12695. https://doi.org/10.1039/D2SC04041G
49. Ingold CK (1933) 266. Significance of tautomerism and of the reactions of aromatic compounds in the electronic theory of organic reactions. J Am Chem Soc (Resumed) (0):1120–1127. https://doi.org/10.1039/JR9330001120
50. Ingold CK (1934) Principles of an electronic theory of organic reactions. Chem Rev 15(2):225–274. https://doi.org/10.1021/cr60051a003
51. Sousa SF, Fernandes PA, Ramos MJ (2007) General performance of density functionals. J Phys Chem A 111(42):10439–10452. https://doi.org/10.1021/jp0734474
52. Morell C, Grand A, Toro-Labbé A (2005) New dual descriptor for chemical reactivity. J Phys Chem A 109(1):205–212. https://doi.org/10.1021/jp046577a
53. Parr RG, Szentpály LV, Liu SB (1999) Electrophilicity index. J Am Chem Soc 121(9):1922–1924. https://doi.org/10.1021/ja983494x
54. Hasija V, Parwaz Khan AA, Sonu KKP, Kaya S, Singh P, Raizada P, Asad M, Rub MA, Alzahrani KA (2024) Dual S-scheme Bi_2MoO_6/g-C_3N_4/Ag_2MoO_4 ternary heterojunction: interfacial charge transfer, broadband spectrum, enhanced redox ability. Solid State Sci 157:107693. https://doi.org/10.1016/j.solidstatesciences.2024.107693
55. Priyadarshi A, Devi HM, Swaminathan R (2023) Disruption of spatial proximities among charged groups in equilibrium-denatured states of proteins tracked using protein charge transfer spectra. Biochemistry 62(11):1643–1658. https://doi.org/10.1021/acs.biochem.3c00006
56. Lu T, Chen QX (2021) Interaction region indicator: a simple real space function clearly revealing both chemical bonds and weak interactions. Chemistry-Methods 1(5):231–239. https://doi.org/10.1002/cmtd.202100007